Published in final edited form as:
Circulation. 2013 January 15; 127(2): 213–223. doi:10.1161/CIRCULATIONAHA.112.131110.

Enhanced Effect of Human Cardiac Stem Cells and Bone Marrow Mesenchymal Stem Cells to Reduce Infarct Size and Restore Cardiac Function after Myocardial Infarction

Adam R. Williams, MD[1,2], **Konstantinos E. Hatzistergos, PhD**[1], **Benjamin Addicott, MD**[1], **Fred McCall, BS**[1], **Decio Carvalho, MD**[1,2], **Viky Suncion, MD**[1], **Azorides R. Morales, MD**[4], **Jose Da Silva, PhD**[1], **Mark A. Sussman, PhD**[5], **Alan W. Heldman, MD**[1,3], and **Joshua M. Hare, MD**[1,3]

[1]Interdisciplinary Stem Cell Institute, University of Miami Miller School of Medicine, Miami, FL

[2]Department of Surgery, University of Miami Miller School of Medicine, Miami, FL

[3]Department of Medicine, University of Miami Miller School of Medicine, Miami, FL

[4]Department of Pathology, University of Miami Miller School of Medicine, Miami, FL

[5]Heart Institute, Department of Biology, San Diego State University, San Diego, CA

Abstract

Background—As mesenchymal stem cells (MSCs) induce proliferation and differentiation of c-kit+ cardiac stem cells (CSCs) in vivo and in vitro, we hypothesized that combining human (h)MSCs with c-kit+ hCSCs produces greater infarct size reduction compared to either cell administered alone after MI.

Methods and Results—Yorkshire swine underwent balloon occlusion of the LAD coronary artery followed by reperfusion, and were immunosuppressed after MI with cyclosporine and methylprednisolone. Intramyocardial injection of either: combination hCSCs/hMSCs (1M/200M, n=5), hCSCs alone (1M, n=5), hMSCs alone (200M, n=5), or placebo (PBS, n=5) was administered to the infarct border zones at 14 days post-MI. Phenotypic response to cell therapy was assessed by cardiac MRI and micromanometer conductance catheterization hemodynamics. While each cell therapy group had reduced MI size relative to placebo ($p<0.05$), the MI size reduction was 2-fold greater in combination vs. either cell therapy alone ($p<0.05$). Accompanying enhanced MI size reduction was substantial improvement in LV chamber compliance (end-diastolic pressure volume relationship, $p<0.01$) and contractility (preload recruitable stroke work and dP/dt_{max}, $p<0.05$) in combination treated swine. EF was restored to baseline in cell treated pigs, while placebo pigs had persistently depressed LV function ($p<0.05$). Immunohistochemistry showed 7-fold enhanced engraftment of stem cells in the combination therapy group vs. either cell type alone ($P<0.001$).

Correspondence: Joshua M. Hare, MD, FACC, FAHA Louis Lemberg Professor of Medicine Director, Interdisciplinary Stem Cell Institute University of Miami Miller School of Medicine Biomedical Research Building / Room 824 PO Box 016960 (R-125) Miami, FL 33101 Phone: 305-243-5579 Fax: 305-243-5584 jhare@med.miami.edu.

Conflict of Interest Disclosures: Drs. Hare and Heldman report owing equity in Vestion, Inc. Vestion did not participate in funding this work. Dr. Hare reports consulting for Kardia, and Drs. Hare and Heldman report receiving research support from Biocardia, Inc.

Conclusions—Combining hMSCs and hCSCs as a cell therapeutic enhances scar size reduction, and restores diastolic and systolic function toward normal after MI. Taken together these findings illustrate important biological interactions between c-kit+ CSCs and MSCs that enhance cell-based therapeutic responses.

Keywords

cardiac stem cells; mesenchymal stem cells; heart failure

Introduction

After myocardial infarction (MI), scar tissue replaces lost myocardium leading to chamber remodeling with depressed left ventricular (LV) systolic and diastolic function; the substrate for heart failure and sudden cardiac death.[1] Historically, the heart had been considered a post-mitotic organ lacking capacity for self-renewal after injury. Observations that adult cardiomyocytes reenter the cell cycle and form new myocytes after MI has challenged long-held dogma that the adult heart is a terminally differentiated organ.[2] The identification of stem cell niches in the adult heart and the ability to isolate c-kit+ cardiac stem cells (CSCs) from a small heart biopsy has generated enormous enthusiasm for the potential to develop safe and effective cell-based therapies to treat ischemic cardiomyopathy.[3,4]

Endogenous proliferation of cardiomyocytes after MI is a rare event and does not lead to full replacement of the large number of lost cells.[5,6] To overcome the limited endogenous regenerative capability of the adult heart, there is intense interest in developing cell-based therapies to promote tissue repair and reverse remodel the injured myocardium. In this regard, several approaches have been employed in which in-vitro cultured stem cells are transplanted into post-MI hearts with the goal of repopulating scar tissue with new cardiomyocytes and ultimately restoring cardiac function. The bone marrow (BM) has been the most widely used source of stem cells to repair the heart, and BM derived mesenchymal stem cells (MSCs) are a particularly attractive candidate due to their multilineage potential, immuno-modulatory properties, and their ability to secrete a host of growth factors which may support endogenous repair mechanisms.[7-9]

Intramyocardial injection of MSCs have been shown to be safe in large animal models and initial data from human trials demonstrate reverse remodeling and improved regional contractility of scarred areas, effects predicted to produce clinical benefits.[10-12] Several mechanisms have been proposed for MSCs to reduce scar size and improve cardiac function in large animal models of MI, including engraftment and differentiation into functional cardiomyocytes,[11] paracrine signaling,[7] and stimulation of endogenous CSC proliferation.[10] Additionally, MSCs have been shown to regulate the hematopoietic stem cell as well as CSC niches.[10,13] More recently, clinical trials reported early results of transplanted cell products prepared from the heart itself. Both the SCIPIO and CADUCEUS trials employed ex vivo amplification of cell preparations from biopsied heart tissue.[14,15] These ex vivo expanded cell products when re-administered to patients improved ejection fraction (EF), reduced MI size, or both.

An optimal cell therapeutic has not yet been identified. Based upon observations that MSCs can promote the formation of stem cell niches in diverse organ systems, we hypothesized that cell-cell interactions could be harnessed for therapeutic purposes, by combining different cell types. To address this hypothesis we tested the prediction that combining human MSCs with CSCs would amplify the phenotypic response of cardiac stem cell therapy by producing greater infarct size reduction and enhanced ventricular performance after MI.

Methods

All animal protocols were reviewed and approved by the University of Miami Institutional Animal Use and Care Committee. The porcine model of MI and intramyocardial stem cell injection was performed as recently described.[16] Briefly, Yorkshire swine (35-40kg) underwent experimental MI followed by stem cell (n=15) or placebo injection (n=5). Cardiac magnetic resonance imaging (CMR) and micromanometer conductance catheter pressure volume (PV) loop analysis was conducted to assess structural and functional changes.[17,18] For all procedures, anesthesia was induced with ketamine (33mg/kg) intramuscular and maintained with inhaled isoflurane 2-4%.

Myocardial infarction

A closed-chest, ischemia-reperfusion protocol to generate a model of anterior wall MI was used. Using angioplasty techniques, balloon occlusion of the left anterior descending coronary artery immediately beyond the first diagonal branch for 90 minutes was performed to induce MI and full reperfusion was confirmed by angiography after balloon deflation. Aspirin 81mg daily was given orally for the duration of study.

Cardiac Magnetic Resonance Imaging

CMR studies were conducted on a Siemens Trio 3T Tim (Erlangen, Germany) scanner with Syngo MR software using a 16-channel body surface coil with ECG gating and short breath-hold acquisitions. All animals underwent CMR at baseline, 2 weeks post MI (pre-injection), 4 weeks post MI, and 6 weeks post MI (pre-sacrifice).

Steady-state free precession (SSFP) cine images in 2-chamber short axis planes (slice thickness 8mm, field of view [FOV] 280-300mm, matrix 192×100, repetition time [TR] 40msec, echo time [TE] 1-2 msec, number of averages 2, band width [BW] 965kHz, flip angle 60 degrees) were obtained. At end-diastole and end-systole, semi-automated epicardial and endocardial borders were drawn in contiguous short axis cine images covering the apex to mitral valve plane using QMass Software (Medis, Leiden, Netherlands) to calculate LV mass, end-diastolic volume (EDV), end-systolic volume (ESV), stroke volume (SV), and EF.

Short axis and 2-chamber long axis delayed enhancement (DE) images (slice thickness of 8mm with no gap, FOV 280-300mm, matrix 256×100, TR/TE 500ms, BW 250kHz, and a flip angle of 20 degrees) were acquired 8 minutes following intravenous infusion of gadolinium 0.3mmol/kg. Scar size was calculated from the short axis DE images covering the apex to the mitral valve plane. Using QMass software, epicardial and endocardial contours of the LV were drawn with a semi-automated tool. The signal intensity of normal and scarred myocardium was calculated by the software, and infarct size quantified by full-width at half-maximum intensity.

Cell isolation and culturing

To obtain c-kit+ hCSCs, explanted cardiac tissue was harvested from the core of apical tissue removed during implantation of a left ventricle assist device (LVAD) in a single human male donor. CSCs expressing c-kit were isolated from enzymatic dissociated myocardial sample using magnetic microbeads coupled with specific (anti-human CD117) antibodies. After dissociation, cells were plated at high density, amplified, harvested, and cryopreserved. A BM aspirate was obtained from the iliac crest of a human male donor to obtain hMSCs. hMSCs were isolated from other BM cells by Ficoll density centrifugation and plastic adherence as previously described;[19] hMSCs were amplified, harvested, and cryopreserved. Iron oxide (Molday ION, BioPal, Worchester, MA) was used to label cells

for imaging with CMR as recently described.[20] Iron oxide experiments were performed in additional animals (n=2) to detect accurate delivery and retention; thus, did not affect the main results of the cell comparisons.

Thoracoscopy guided intramyocardial injection

At 14 days post-MI, animals underwent thoracoscopy guided direct transepicardial stem cell (hCSC/hMSC, n=5; hMSC, n=5; hCSC, n=5) or placebo injection (n=5). A left mini-thoracotomy was created with a small 4-5 cm incision in the 5th anterior/lateral intercostal space, and the left plural cavity entered under direct visualization. A 5mm port was placed in the 6th or 7th intercostal space, and a 5mm endoscope (Karl Storz, Tuttlingen, Germany) inserted into the left chest cavity. The pericardium was opened and infarct area identified by wall motion abnormalities and correlation with coronary anatomy. A curved 27-guage needle was inserted tangentially into the myocardium and 10 separate injections administered to the infarct border zone. A 12-French chest tube was inserted into the left pleural cavity via the port incision, and tunneled through the chest wall. All incisions were closed and the chest tube placed to −20cm of underwater suction to evacuate the pnuemothorax. Fluoroscopy was done to confirm lung expansion and the chest tube removed prior to extubation. Animals were recovered and provided adequate post-operative analgesia with a transdermal fentanyl patch (75mcg/hr) for 3 days and bupernorpherine (0.03mg/kg IM) immediately post-procedure.

On the morning of stem cell injection, cells were thawed, washed and resuspended in phosphate buffered saline (PBS). For hMSC alone injections, 200 million hMSCs were suspended in 6ml of PBS, and for hCSC alone injection, 1 million hCSCs were suspended in 3 ml of PBS. For the combination c-kit+ hCSC / hMSC injections, 1 million hCSCs and 200 million hMSCs were suspended in 6 ml of PBS and mixed before injection. For placebo injections, 6ml of PBS was administered. All cells or placebo injections were divided into 10 equal volume aliquots and injected transepicardially with a 27-gauge needle. All animals were euthanized at 6 weeks post MI.

Micromanometer conductance catheterization

Left ventricle invasive PV loops were obtained immediately before intramyocardial stem cell or placebo injection and at 4-weeks post injection to assess hemodynamic changes. A PV loop transducer (Millar Instruments Inc., Houston, TX) was zeroed and balanced in warm saline and guided to the LV apex by fluoroscopy via a peripheral artery introducer with the chest closed. Steady-state PV loops were acquired during a short breath hold. A Fogarty balloon was guided through the venous introducer to the inferior vena cava (IVC) / right atrium junction and inflated to occlude lower body venous return to the heart, while recording a series of occlusion PV loops during a short breath hold. The PV loop volumes were calibrated to corresponding CMR derived EDV and SV using the point-and-difference technique, which calibrates the conductance volume signal to the independently obtained CMR volume assessment.[16]

Histology

Hearts were fixed for >24h in 10% buffered formalin and sliced transversely into 4mm thick slices using a commercial meat cutter. Slices 4, 5, 6, 7 and 8 were embedded in paraffin (FFPE) and processed for confocal analysis. Engraftment of human stem cells in swine hearts was assessed using DNA fluorescence in situ hybridization (FISH), using a FISH probe specific for the human Alu repetitive DNA elements. Immunofluorescence co-staining was performed using: anti-porcine c-kit [mouse monoclonal, clone 2B8/BM, kindly provided by Dr. Revilla], anti-human c-kit (rabbit polyclonal, c-kit PharDx; DAKO, Carpinteria, CA), and tropomyosin (mouse monoclonal, Abcam, Cambridge, MA)

antibodies. Representative samples were selected from the infarct zone (IZ), left and right border zones (BZ) containing infarct along with non-scarred tissue, and remote zone (RZ) obtained from the posterior non-infarcted LV wall for engraftment quantification. The total number of positively stained cells were quantified per slide to calculate the number of cells per unit volume (cm^3) from each sample. Morphometric analyses were performed with a custom research package (Image J, NIH, Bethesda, Maryland). Microscopic evaluations and image acquisitions were performed with a Zeiss LSM-710 Confocal Microscope (Carl Zeiss MicroImaging, Thornwood, NY).

Immune suppression

All swine, cell treated and placebo, were placed on cyclosporine and methylprednisolone therapy to prevent rejection of human stem cell transplants. Twelve days post MI, animals were started on cyclosporine 400mg PO twice daily. Serum trough levels were measured at least once per week and titrated to maintain a serum level of 125-225ng/ml. Methylprednisolone 250mg IM was administered the morning of intramyocardial injection (14 days post MI) and tapered to 125mg PO daily over the first two weeks post-transplant and all animals were continued on that dose for the duration of the study.

Statistics

The impact of cell therapy on phenotypic changes measured over time was evaluated using ANOVA with repeated measures. Time post-injection was used as the repeated factor and differences within groups were described at each time point. Multiple testing between groups in the repeated measures ANOVA models utilized a Bonferroni correction; actual p-values are reported and unadjusted. Pre-injection versus post-injection PV loop hemodynamic parameters were compared with paired Student's t-test. Statistics were assessed using SAS Software (Version 9.2; Cary, NC) and GraphPad Prism (Version 4.03; La Jolla, CA) was used to plot graphs. All values are expressed as means (+/-SD) unless otherwise stated. A p-value of less than 0.05 was considered statistically significant.

Results

Infarct size reduction and restoration of EF after stem cell injection

Global changes in LV function, chamber dimensions, and scar size are summarized in Table I. Delayed enhancement CMR was used to measure changes in absolute scar mass as well as infarct size as a percentage of LV mass. Two-weeks after MI, prior to injection, scar size was similar in all groups ($p=0.811$) and encompassed approximately 18% of the left ventricular mass (Table I). All stem cell treated groups had significant reductions in the infarct size 4-weeks following cell injection, while the placebo injected group had unchanged infarct size from 2 to 6 weeks post MI (Figure 1). While ckit+ hCSC alone and hMSC alone therapy had comparable infarct size reductions (absolute scar mass) of 10.4±2.6% ($p=0.010$) and 9.9±1.7% ($p=0.013$), respectively, at 4 weeks after cell therapy, the combination of hCSC/hMSC produced a 2-fold greater reduction in scar mass of 21.1±5.0% ($p<0.0001$). Furthermore, the infarct size measured as a percentage of LV mass decreased 36.8±3.3% in combination hCSC/hMSC treated animals ($p<0.0001$), 25.6±3.2% in the hCSC alone group ($p<0.0001$), 23.6±4.4% in the hMSC alone group ($p<0.0001$), and 10.9±4.2% in the placebo group ($p=0.036$). Infarct size reduction by absolute mass was significantly greater in the combination hCSC/hMSC group compared to hCSC alone ($p=0.035$), hMSC alone ($p=0.033$), and placebo ($p=0.0002$). hCSC ($p=0.026$) and hMSC ($p=0.030$) had improved scar size reduction compared to placebo. The change in scar size between hCSC alone and hMSC alone were not different ($p=0.964$).

EF prior to MI was approximately 40%, consistent with previous studies in Yorkshire swine,[10] and similar between groups (p=0.412; Table 1). Two weeks after MI, EF decreased approximately 20% from baseline (Figure 2A). Interestingly, EF returned to baseline levels by 4-weeks post-injection in combination hCSC/hMSC (p=0.001), hCSC alone (p<0.001) and hMSC (p<0.001) treated groups, while remaining persistently depressed in placebo treated animals (p=0.885) (Figure 2A). Correlation of the percentage change in EF relative to the percentage change in EDV (Figure 2B) and ESV (Figure 2C) showed attenuation of remodeling in all stem cell treated pigs compared to the placebo treated animals, and was most pronounced in the combination hCSC / hMSC group. Furthermore, placebo treated animals had significantly increased EDV (p=0.018) from 2 weeks post-MI (pre-injection) to 6 weeks post-MI (Figure 2B).

Hemodynamic changes after stem cell injection

Next we assessed the impact of cell-therapy on LV diastolic and systolic performance, measured with conductance micromanometer catheterization before stem cell injection and 4-weeks post injection. Pre-injection hemodynamic parameters were similar in all groups.

The end diastolic pressure volume relationship (EDPVR), a measure of ventricular diastolic compliance, improved in the combination hCSC/hMSC (p=0.005) and hMSC alone (p=0.038) treated animals, consistent with improved LV chamber compliance. Furthermore, EDPVR in combination treated hCSC/hMSC therapy was significantly better compared to placebo at 4-weeks post-injection (Figure 3E). A flatter curve (smaller slope) showed that for any end-diastolic volume the heart functioned at a lower end diastolic pressure (Figure 3C&D). Isovolumetric relaxation time, measured by tau and an index of active ventricular relaxation, was also significantly lower at 4-weeks post-injection in the combination c-kit+ hCSC / hMSC group as well as the c-kit+ hCSC group compared to placebo (Figure 3F). Additionally, the combination therapy group had significantly improved rate of pressure change during diastole (dP/dt_{min}) at 4-weeks post-injection compared to all other cell-therapy and placebo treated groups (Figure 3G). Taken together, these hemodynamic changes suggest that combining hMSCs with ckit+ hCSCs significantly improves diastolic function to the greatest degree after MI, affecting both active and passive phases of diastolic relaxation.

There was no change in measures of preload or afterload in any of the groups, with the exception of larger EDV in the hCSC alone group (Figure 4B); however, EDV measured by CMR showed no difference in the c-kit+ alone treated group (Table 1). The combination hCSC/hMSC treated group demonstrated improved measures of contractility, including the maximal rate of pressure change during systole (dP/dt_{max}) (Figure 4D; p=0.018) and preload recruitable stroke work (PRSW) (Figure 4E; p=0.001); and, interestingly, the hMSC alone group also showed improvements in PRSW as well (Figure 4E; p=0.024).

Integrated measures of cardiac performance—EF, cardiac output (CO), stroke volume (SV), stroke work (SW), and heart rate (HR)—integrate all the measures of contractility, preload, afterload, and lusitropy. All stem cell treated groups demonstrated improved EF and SV (Figure 5A&B). Stroke work (Figure 5C) improved in the combination hCSC / hMSC group (p=0.023) and hMSC alone group (p=0.023). Cardiac output (Figure 5D) improved in hCSC alone (p=0.015) and hMSC alone (p=0.018), and had a trend towards improvement in the combination therapy group (p=0.064). Heart rate was unchanged in all the groups (Figure 5E; p=NS).

Engraftment and host immune response to transplanted human cells

All groups had similar therapeutic cyclosporine trough levels throughout the study (178.3±19.4 vs. 233.6±40.0 vs. 225.2±52.6 vs. 183.1±12.1; combination hCSC/MSC vs. hCSC alone vs. hMSC alone vs. placebo, respectively; p=0.55), and all were treated with methylprednisolone per protocol. Post-mortem tissue samples were taken from serial sections of each heart; and a cardiac pathologist analyzed hematoxylin and eosin (H&E) and Masson's trichrome stained sections from the IZ, BZ and RZ (30 specimens per heart) from each animal. All animals showed structural changes of post-reperfusion necrosis, including stages of fibrosis, vascular proliferation and foci of calcification, which could occasionally be identified as calcified cardiomyocytes. There was minimal evidence of rejection of human stem cells (administered in combination or alone) as demonstrated by the presence of rare, small lympho-reticular aggregates in all groups. Interestingly, one animal in the combination hCSC/hMSC group and one animal in the hMSC alone group had prominent foci of nodular lympho-reticular aggregates. Additionally, one animal in the placebo treated group had diffuse mononuclear cell infiltrate.

CMR imaging was used to detect retention of injected human stem cells labeled with iron oxide and confirmed appropriate delivery of cells (Figure 6A-G). Engraftment of human stem cells in swine myocardium was assessed using confocal immunoflurorescence. Clusters of hCSCs and hMSCs were localized in the IZ and BZ by immunohistochemical staining for Alu, an antibody that binds to a specific sequence of DNA found only in human cells but not swine cells (Figure 6H). Additionally, transplanted human stem cells engrafted into vessels (Figure 6I). Corresponding H&E histology and gross section showed no evidence of host inflammatory response to engrafted human stem cells (Figure 6J&K). The engraftment of hCSCs and hMSCs in the combination group was 7-fold greater than in either cell group administered alone (Figure 6L).

Discussion

Here, we show that hMSCs and c-kit+ hCSCs reduce infarct size and improve LV function in post-MI swine. When both cells are injected together, there is a 2-fold greater reduction in scar size compared to either cell administered alone. Scar size reduction in all stem cell treated pigs was accompanied by substantial recovery in cardiac diastolic and systolic function, which was not as robust when either cell was administered alone. Taken together, intramyocardial injection of hMSCs with hCSCs as a combined cell therapeutic enhances scar size reduction and improves hemodynamic function in post-MI swine, suggesting that this combination represents an effective and robust cell therapeutic strategy. The improvement in both structural and functional parameters has important clinical implications for the use of this combination therapeutic for heart failure.

The quest for the ideal cell based therapeutic strategy is intensifying. Following encouraging preclinical models, the field has recently transitioned to the conduct of early phase clinical trials. Strategies have included the use of both mesenchymal cells from a variety of tissue sources (BM, adipose)[9] and CSCs obtained from myocardial specimens.[12,14] Recent mechanistic insights that MSCs stimulate CSC recruitment and lineage commitment suggest that combining cells may offer therapeutic advantages and could overcome factors inhibiting or offsetting the efficacy of current approaches.[10]

In terms of functional improvement in LV performance, we showed that all stem cell treated animals had recovery of EF to near baseline level, while the placebo treated animals had persistently depressed LV function. Accordingly, EF may not be the optimal metric to assess outcomes after cell-based therapy. Previously, we demonstrated in humans with ischemic cardiomyopathy that intramyocardial injection of BM derived stem cells dramatically

reduced LV chamber sizes in parallel, thus, obscuring improvements in global EF.[12] Accompanying this reverse remodeling seen in humans was improved regional contractility of the treated scar. Therefore, assessing metrics for scar size and chamber dimensions as well as specific measures of cardiac function, such as contractility and lusitropy, may provide better insight to the clinical effects of stem cells on scarred myocardium.

In order to assess more detailed analysis of LV function, we conducted micromanometer conductance catheter PV loop measurements to assess the impact of stem cell therapy on hemodynamic performance. While all stem cell treated groups had improved measures of integrated cardiac performance (EF, SW, and CO), specific measures of contractility, such as PRSW and dP/dt_{max}, were preferentially improved in the combination hMSC/hCSC therapy. In addition to systolic impairment, diastolic dysfunction is an additional hallmark of the post infarction LV.[21-23] Important measures of passive and active diastolic performance, such as LV chamber compliance (the slope of the EDPVR), isovolumetric relaxation time (tau), and minimal rate of pressure change (dP/dt_{min}) can be accurately measured with PV loops. In the combination hMSC/hCSC group we demonstrated improved LV compliance after therapy as well as improved rate of pressure change during diastole compared to all other groups (Figure 3). This improved lusitropy and contractility with combination therapy suggests a complementary effect of hCSCs and hMSCs on hemodynamic performance. Moreover, the salutary effects of this cell combination on both phases of the cardiac cycle, coupled with enhanced reduction in the burden of myocardial scar, auger well for the possibility that this combination could yield meaningful clinical benefits in patients.

Differentiation of MSCs and CSCs into adult cardiomyocytes and new blood vessels has been proposed as a potential mechanism of action to repopulate scar tissue after MI.[11,24] Previous studies in swine demonstrated that intramyocardial injection of MSCs may also stimulate endogenous CSCs to regenerate myocardium via cell-cell interactions and stimulation of cardiomyocyte cell cycling.[10] Furthermore, paracrine signaling likely plays an important role in stem cell therapy as it has been shown that MSCs secrete an array of growth factors, cytokines, and matrix metalloproteinases that that may stimulate endogenous repair mechanisms and reverse remodeling.[7] Indeed, the mechanism of action of stem cell therapy remains controversial and likely numerous cell actions work in concert to improve cardiac structure and function after MI.

Emerging data from clinical trials of stem cell therapy for heart failure support the potential of regenerative medicine as a new treatment modality.[12,14,25] Concurrent with ongoing human studies, experimental animal models of cell therapy are crucial for detailed cardiac phenotyping and delineation of the biological effects of cells on important clinical outcomes. Human stem cell studies in animals have been mostly limited to genetically altered rodent models that allow tolerance to xenotransplantation.[24,26] Swine are a well accepted large animal model for preclinical studies for regulatory approval,[16] but their competent immune system makes xenotransplantation of human cells challenging. To address this, we developed an immunosuppressed swine model to provide a tolerant environment for human stem cell transplantation. An extensive post-mortem review of each heart demonstrated minimal host inflammatory response to the transplanted human cells (Figure 6). Since all animals (placebo and stem cell treated) were administered the same immunosuppression therapy, any effects of the medications would be expected to manifest in the stem cell and placebo groups equally. Importantly, corticosteroid and cyclosporine therapy has been shown to have no effect on infarct size after MI.[27,28]

Our study has important translational implications for cell-based therapy in post-MI patients. hMSCs and c-kit+ hCSCs are adult stem cells easily isolated from a minimally invasive BM biopsy[19] and cardiac endomyocardial biopsy,[4] respectively. Recently, it has been shown that

functional hCSCs can even be isolated from advanced heart failure patients.[4] We have shown that combining c-kit+ hCSCs with hMSCs provides substantial enhancement to scar size reduction as well improved hemodynamic function after MI. These improvements seen in a large animal model of MI would be predicted to provide similar effects in humans with ischemic cardiomyopathy, and immunosuppression may not be necessary if autologous cells are used. As the stem cell field advances, it may become apparent that using a single stem cell to treat the failing heart is not the optimal cell-based strategy, but rather mixtures of complementary cells that provide synergistic effects may enhance therapeutic outcomes. Injecting a mixture of stem cells to damaged myocardium represents a new paradigm in the application of regenerative medicine to advanced heart failure.

Limitations

The major limitation of this study was lack of dose escalation of each stem cell therapy. Previous work by our group has shown that higher dose MSC therapy (200 million cells) provides significantly greater improvements in cardiac function and scar size than low dose MSC therapy (20 million cells) in post-MI swine;[29] thus, our standard dose for MSC therapy is 200 million cells. The optimal dose for CSC therapy as well as when mixed with MSCs remains undefined and requires further investigation. Additionally, iron oxide labeling of cells for retention studies with CMR imaging may be confounded by efflux of iron oxide out of transplanted cells.[30] The iron oxide debris can be engulfed by macrophages; thus, limiting the reliability of long-term imaging with iron oxide labeling for cell retention.

Conclusion

Intramyocardial injection of hMSCs with c-kit+ hCSCs enhances scar size reduction after MI, restoring diastolic and systolic function towards normal. Taken together these findings illustrate the important interactions of hMSCs and c-kit+ hCSCs that result in substantial enhancement to cell-based therapy after MI. These findings have important clinical implications for future investigations of cell therapy for heart disease.

Acknowledgments

The investigators would like to thank Adam Mendizabal, MS for statistical contributions; and Ray Gonzalez, Jose Rodriguez, David Valdes, and Marcos Rosado for their technical contributions.

Funding Sources: Dr. Hare is funded by National Institutes of Health grants U54-HL081028 (Specialized Center for Cell Based Therapy), P20-HL101443, and RO1-grants HL084275, HL110737-01, HL107110, and HL094849.

References

1. Pfeffer MA, Braunwald E. Ventricular remodeling after myocardial infarction. Experimental observations and clinical implications. Circulation. 1990; 81:1161–72. [PubMed: 2138525]
2. Beltrami AP, Urbanek K, Kajstura J, Yan SM, Finato N, Bussani R, Nadal-Ginard B, Silvestri F, Leri A, Beltrami CA, Anversa P. Evidence that human cardiac myocytes divide after myocardial infarction. N Engl J Med. 2001; 344:1750–7. [PubMed: 11396441]
3. Bearzi C, Rota M, Hosoda T, Tillmanns J, Nascimbene A, De AA, Yasuzawa-Amano S, Trofimova I, Siggins RW, Lecapitaine N, Cascapera S, Beltrami AP, D'Alessandro DA, Zias E, Quaini F, Urbanek K, Michler RE, Bolli R, Kajstura J, Leri A, Anversa P. Human cardiac stem cells. Proc Natl Acad Sci U S A. 2007; 104:14068–73. [PubMed: 17709737]
4. D'Amario D, Fiorini C, Campbell PM, Goichberg P, Sanada F, Zheng H, Hosoda T, Rota M, Connell JM, Gallegos RP, Welt FG, Givertz MM, Mitchell RN, Leri A, Kajstura J, Pfeffer MA, Anversa P. Functionally competent cardiac stem cells can be isolated from endomyocardial biopsies of patients with advanced cardiomyopathies. Circ Res. 2011; 108:857–61. [PubMed: 21330601]

5. Zeng L, Hu Q, Wang X, Mansoor A, Lee J, Feygin J, Zhang G, Suntharalingam P, Boozer S, Mhashilkar A, Panetta CJ, Swingen C, Deans R, From AH, Bache RJ, Verfaillie CM, Zhang J. Bioenergetic and functional consequences of bone marrow-derived multipotent progenitor cell transplantation in hearts with postinfarction left ventricular remodeling. Circulation. 2007; 115:1866–75. [PubMed: 17389266]

6. Xiong Q, Ye L, Zhang P, Lepley M, Swingen C, Zhang L, Kaufman DS, Zhang J. Bioenergetic and functional consequences of cellular therapy: activation of endogenous cardiovascular progenitor cells. Circ Res. 2012; 111:455–68. [PubMed: 22723295]

7. Gnecchi M, Zhang Z, Ni A, Dzau VJ. Paracrine mechanisms in adult stem cell signaling and therapy. Circ Res. 2008; 103:1204–19. [PubMed: 19028920]

8. Pittenger MF, Mackay AM, Beck SC, Jaiswal RK, Douglas R, Mosca JD, Moorman MA, Simonetti DW, Craig S, Marshak DR. Multilineage potential of adult human mesenchymal stem cells. Science. 1999; 284:143–7. [PubMed: 10102814]

9. Williams AR, Hare JM. Mesenchymal stem cells: biology, pathophysiology, translational findings, and therapeutic implications for cardiac disease. Circ Res. 2011; 109:923–40. [PubMed: 21960725]

10. Hatzistergos KE, Quevedo H, Oskouei BN, Hu Q, Feigenbaum GS, Margitich IS, Mazhari R, Boyle AJ, Zambrano JP, Rodriguez JE, Dulce R, Pattany PM, Valdes D, Revilla C, Heldman AW, McNiece I, Hare JM. Bone marrow mesenchymal stem cells stimulate cardiac stem cell proliferation and differentiation. Circ Res. 2010; 107:913–22. [PubMed: 20671238]

11. Quevedo HC, Hatzistergos KE, Oskouei BN, Feigenbaum GS, Rodriguez JE, Valdes D, Pattany PM, Zambrano JP, Hu Q, McNiece I, Heldman AW, Hare JM. Allogeneic mesenchymal stem cells restore cardiac function in chronic ischemic cardiomyopathy via trilineage differentiating capacity. Proc Natl Acad Sci U S A. 2009; 106:14022–7. [PubMed: 19666564]

12. Williams AR, Trachtenberg B, Velazquez DL, McNiece I, Altman P, Rouy D, Mendizabal AM, Pattany PM, Lopera GA, Fishman J, Zambrano JP, Heldman AW, Hare JM. Intramyocardial stem cell injection in patients with ischemic cardiomyopathy: functional recovery and reverse remodeling. Circ Res. 2011; 108:792–6. [PubMed: 21415390]

13. Mendez-Ferrer S, Michurina TV, Ferraro F, Mazloom AR, Macarthur BD, Lira SA, Scadden DT, Ma'ayan A, Enikolopov GN, Frenette PS. Mesenchymal and haematopoietic stem cells form a unique bone marrow niche. Nature. 2010; 466:829–34. [PubMed: 20703299]

14. Bolli R, Chugh AR, D'Amario D, Loughran JH, Stoddard MF, Ikram S, Beache GM, Wagner SG, Leri A, Hosoda T, Sanada F, Elmore JB, Goichberg P, Cappetta D, Solankhi NK, Fahsah I, Rokosh DG, Slaughter MS, Kajstura J, Anversa P. Cardiac stem cells in patients with ischaemic cardiomyopathy (SCIPIO): initial results of a randomised phase 1 trial. Lancet. 2011; 378:1847–57. [PubMed: 22088800]

15. Makkar RR, Smith RR, Cheng K, Malliaras K, Thomson LE, Berman D, Czer LS, Marban L, Mendizabal A, Johnston PV, Russell SD, Schuleri KH, Lardo AC, Gerstenblith G, Marban E. Intracoronary cardiosphere-derived cells for heart regeneration after myocardial infarction (CADUCEUS): a prospective, randomised phase 1 trial. Lancet. 2010; 379:895–904. [PubMed: 22336189]

16. McCall FC, Telukuntla KS, Karantalis V, Suncion VY, Heldman AW, Mushtaq M, Williams AR, Hare JM. Myocardial infarction and intramyocardial injection models in swine. Nat Protoc. 2012; 7:1479–96. [PubMed: 22790084]

17. Amado LC, Schuleri KH, Saliaris AP, Boyle AJ, Helm R, Oskouei B, Centola M, Eneboe V, Young R, Lima JA, Lardo AC, Heldman AW, Hare JM. Multimodality noninvasive imaging demonstrates in vivo cardiac regeneration after mesenchymal stem cell therapy. J Am Coll Cardiol. 2006; 48:2116–24. [PubMed: 17113001]

18. Amado LC, Saliaris AP, Schuleri KH, St JM, Xie JS, Cattaneo S, Durand DJ, Fitton T, Kuang JQ, Stewart G, Lehrke S, Baumgartner WW, Martin BJ, Heldman AW, Hare JM. Cardiac repair with intramyocardial injection of allogeneic mesenchymal stem cells after myocardial infarction. Proc Natl Acad Sci U S A. 2005; 102:11474–9. [PubMed: 16061805]

19. Lennon DP, Caplan AI. Isolation of human marrow-derived mesenchymal stem cells. Exp Hematol. 2006; 34:1604–5. [PubMed: 17046583]

20. Addicott B, Willman M, Rodriguez J, Padgett K, Han D, Berman D, Hare JM, Kenyon NS. Mesenchymal stem cell labeling and in vitro MR characterization at 1.5 T of new SPIO contrast

agent: Molday ION Rhodamine-B. Contrast Media Mol Imaging. 2011; 6:7–18. [PubMed: 20690161]

21. De MS, Thomas JD, Greenberg NL, Vandervoort PM, Verdonck PR. Assessment of the time constant of relaxation: insights from simulations and hemodynamic measurements. Am J Physiol Heart Circ Physiol. 2001; 280:H2936–H2943. [PubMed: 11356655]
22. Kawaji K, Codella NC, Prince MR, Chu CW, Shakoor A, LaBounty TM, Min JK, Swaminathan RV, Devereux RB, Wang Y, Weinsaft JW. Automated segmentation of routine clinical cardiac magnetic resonance imaging for assessment of left ventricular diastolic dysfunction. Circ Cardiovasc Imaging. 2009; 2:476–84. [PubMed: 19920046]
23. Nagueh SF, Middleton KJ, Kopelen HA, Zoghbi WA, Quinones MA. Doppler tissue imaging: a noninvasive technique for evaluation of left ventricular relaxation and estimation of filling pressures. J Am Coll Cardiol. 1997; 30:1527–33. [PubMed: 9362412]
24. Beltrami AP, Barlucchi L, Torella D, Baker M, Limana F, Chimenti S, Kasahara H, Rota M, Musso E, Urbanek K, Leri A, Kajstura J, Nadal-Ginard B, Anversa P. Adult cardiac stem cells are multipotent and support myocardial regeneration. Cell. 2003; 114:763–76. [PubMed: 14505575]
25. Hare JM, Fishman JE, Gerstenblith G, Difede Velazquez DL, Zambrano JP, Suncion VY, Tracy M, Ghersin E, Johnston PV, Brinker JA, Breton E, Davis-Sproul J, Schulman IH, Byrnes J, Mendizabal AM, Lowery MH, Rouy D, Altman P, Wong Po FC, Ruiz P, Amador A, Da SJ, McNiece IK, Heldman AW. Comparison of allogeneic vs autologous bone marrow-derived mesenchymal stem cells delivered by transendocardial injection in patients with ischemic cardiomyopathy: The POSEIDON randomized trial. JAMA. 2012:1–11.
26. Toma C, Pittenger MF, Cahill KS, Byrne BJ, Kessler PD. Human mesenchymal stem cells differentiate to a cardiomyocyte phenotype in the adult murine heart. Circulation. 2002; 105:93–8. [PubMed: 11772882]
27. Karlsson LO, Zhou AX, Larsson E, Astrom-Olsson K, Mansson C, Akyurek LM, Grip L. Cyclosporine does not reduce myocardial infarct size in a porcine ischemia-reperfusion model. J Cardiovasc Pharmacol Ther. 2010; 15:182–9. [PubMed: 20435992]
28. Vogel WM, Zannoni VG, Abrams GD, Lucchesi BR. Inability of methylprednisolone sodium succinate to decrease infarct size or preserve enzyme activity measured 24 hours after coronary occlusion in the dog. Circulation. 1977; 55:588–95. [PubMed: 837501]
29. Schuleri KH, Feigenbaum GS, Centola M, Weiss ES, Zimmet JM, Turney J, Kellner J, Zviman MM, Hatzistergos KE, Detrick B, Conte JV, McNiece I, Steenbergen C, Lardo AC, Hare JM. Autologous mesenchymal stem cells produce reverse remodelling in chronic ischaemic cardiomyopathy. Eur Heart J. 2009; 30:2722–32. [PubMed: 19586959]
30. Kraitchman DL, Heldman AW, Atalar E, Amado LC, Martin BJ, Pittenger MF, Hare JM, Bulte JW. In vivo magnetic resonance imaging of mesenchymal stem cells in myocardial infarction. Circulation. 2003; 107:2290–3. [PubMed: 12732608]

Clinical Impact

Stem cell and cell-based therapy represent a potentially transformative new therapy for left ventricular dysfunction and other cardiovascular diseases. Bone marrow mesenchymal stem cells (MSCs) and cardiac stem cells (CSCs) are two of the leading candidates for cellular cardiomyoplasty. Based on earlier observations that MSCs interact with and promote survival and lineage commitment of CSCs, we tested whether combining MSCs with CSCs would augment a therapeutic response relative to either cell alone. Using xenotransplantation of human MSCs and c-kit+ CSCs delivered intramyocardially to swine following myocardial infarction (MI), we show that combining MSCs and CSCs enhances greatly the reduction in infarct size and improvement in LV diastolic and systolic function achieved with either cell alone. These data support the idea that cell combination therapy is a practical and effective strategy to improve responses to cell therapy, and support the conduct of clinical trials testing co-injection of MSCs and CSCs in humans with cardiac injury due to MI and possibly other sources of LV dysfunction.

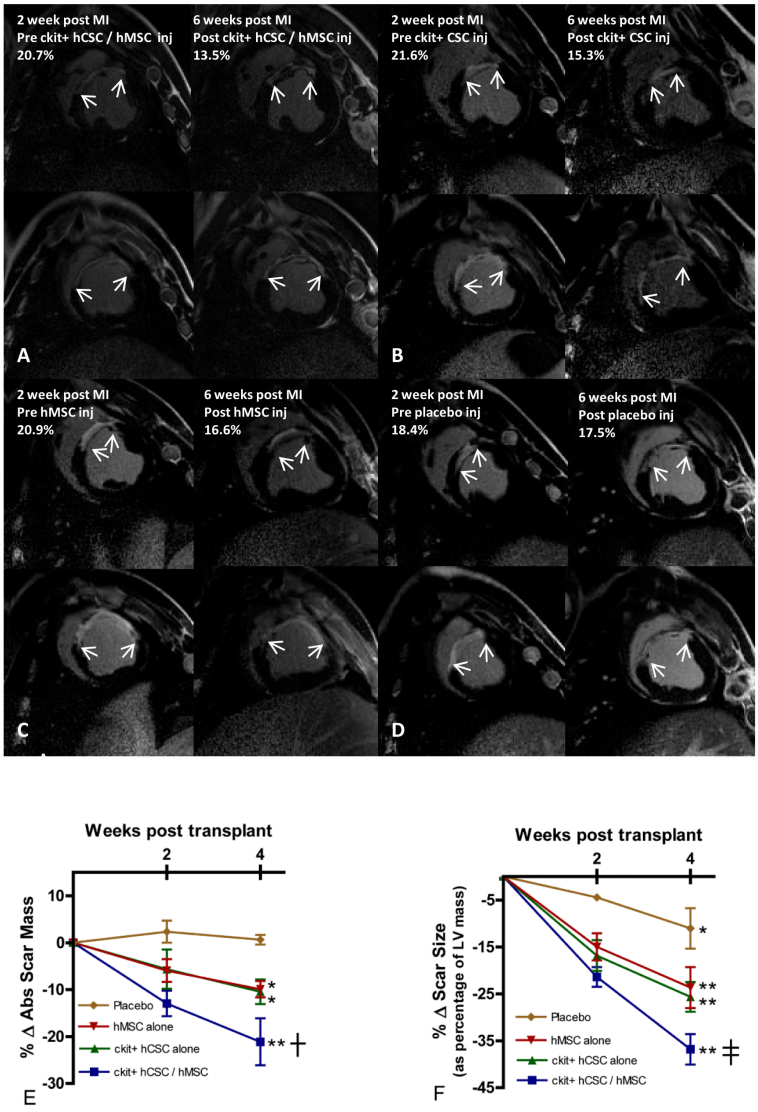

Figure 1.

Infarct size reduction after hCSC and bone marrow hMSC therapy. Delayed enhancement CMR images showing pre-injection scar and 4-weeks post-injection scar changes (white arrows indicate infarct extension) in (A) combination c-kit+ hCSC/hMSC (n=5), (B) c-kit+ hCSC alone (n=5), (C) hMSC alone (n=5), and (D) placebo (n=5) treated pigs. Reduction in (E) absolute infarct size and (F) infarct size as a percentage of LV mass shows all stem cell treated pigs had reduced infarct size compared to placebo and combination therapy had substantially greater scar size reduction compared to either hMSC alone or hCSC alone. (*p<0.05 and **p<0.0001 within group repeated measures ANOVA; †p<0.05 combination hCSC/hMSC vs. both hCSC alone and hMSC alone between group repeated measures ANOVA; ≠. p=0.02 combination hCSC/hMSC vs. hMSC alone and p=0.06 combination hCSC/hMSC vs hCSC alone between group repeated measures ANOVA; graphs represent mean±SEM)

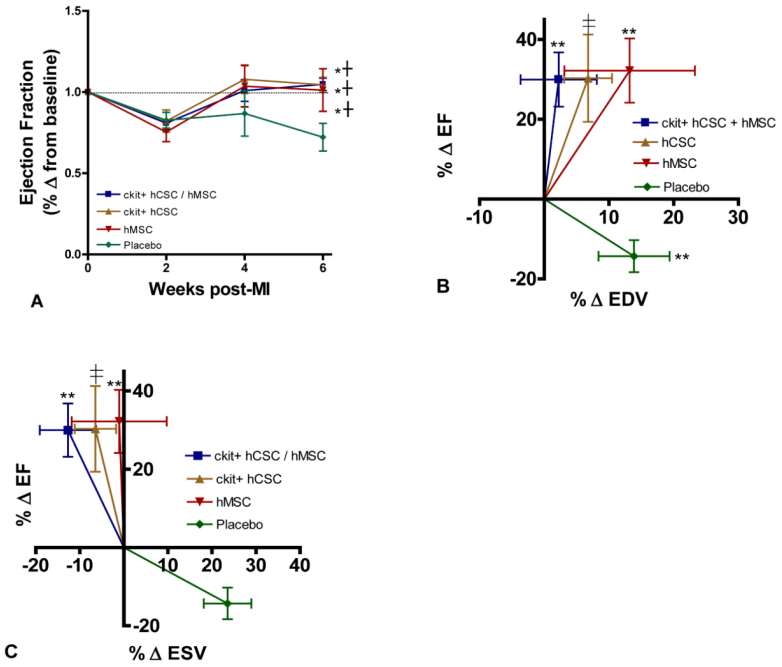

Figure 2.

Restoration of LV function and attenuation of remodeling with hCSC and hMSC therapy. (A) Ejection fraction (EF) was restored to baseline level in combination c-kit+ hCSC/hMSC (n=5), c-kit+ hCSC alone (n=5), and hMSC alone (n=5) treated animals, while remaining depressed in placebo treated animals (n=5) during follow-up. Changes in LVEF plotted against the changes in (B) end-diastolic volume and (C) end-systolic volume at 4-weeks post injection demonstrate attenuation in remodeling with hCSCs and hMSCs compared to placebo, which was more pronounced in combination c-kit+ hCSC and hMSC therapy compared to either cell alone treated groups. (*p<0.01 within group repeated measures ANOVA; **p<0.05 paired t-test pre-injection vs. 4 weeks post-injection; †p<0.05 vs. placebo between group repeated measures ANOVA; ≠p=0.06 paired t-test pre-injection vs. 4 weeks post-injection; graphs represent mean±SEM)

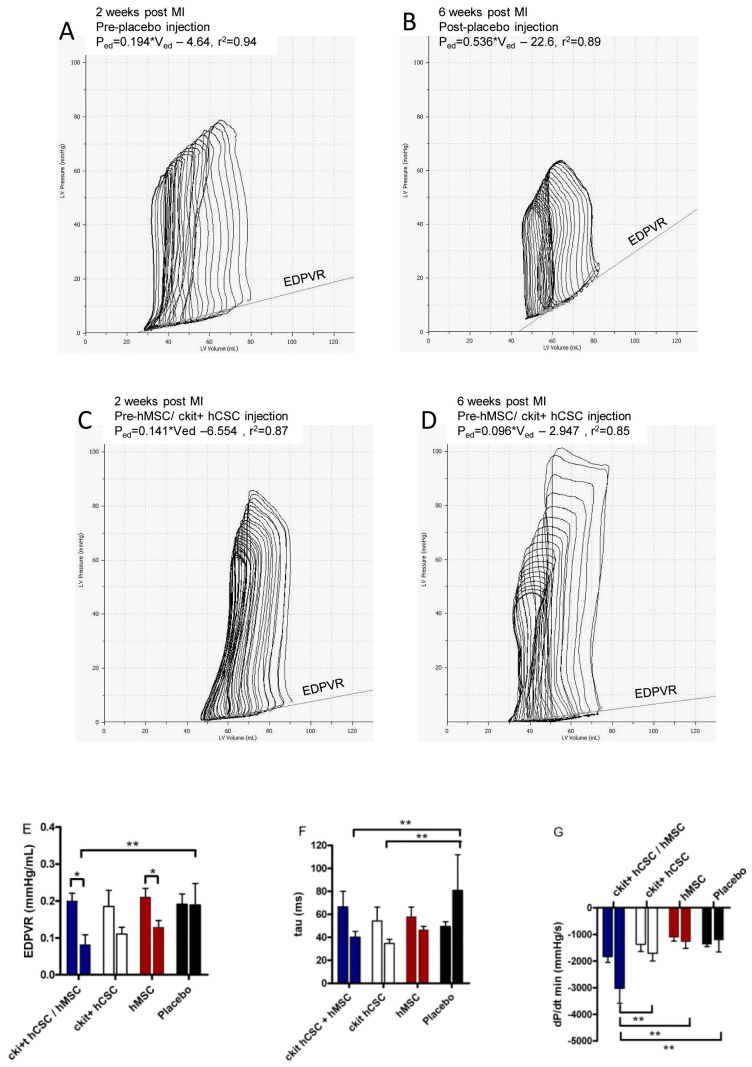

Figure 3.

Impact of hCSC and hMSC therapy on diastolic function. (A) Example of a placebo treated animal before injection vs. (B) post-injection end-diastolic pressure volume relationship (EDPVR) shows a significant rise in slope, indicating that for any given end-diastolic volume the heart operates at an increased end-diastolic pressure. (C) Example of a combination hCSC and hMSC treated animal before injection vs. (D) 4-weeks post-injection depicting lower end-diastolic pressures for any given end-diastolic volume, indicating improved LV chamber compliance. Also shown in the PV loop curves is lower EDP after hCSC/MSC therapy as well as improvements in other hemodynamic parameters such as increased stroke work (area in curve), and increased developed pressure (ESP-EDP) 4-weeks after human stem cell therapy. Graphs showing (E) the slope of the regression curve for EDPVR, (F) tau, the isovolumetric relaxation time, and (G) dP/dtmin, the rate of pressure change during diastole. All graphs show pre-injection (2-weeks post-MI) vs. 4-weeks post-injection values. (*p<0.05 paired t-test, **p<0.05 between group repeated measures ANOVA; graphs represent mean±SEM)

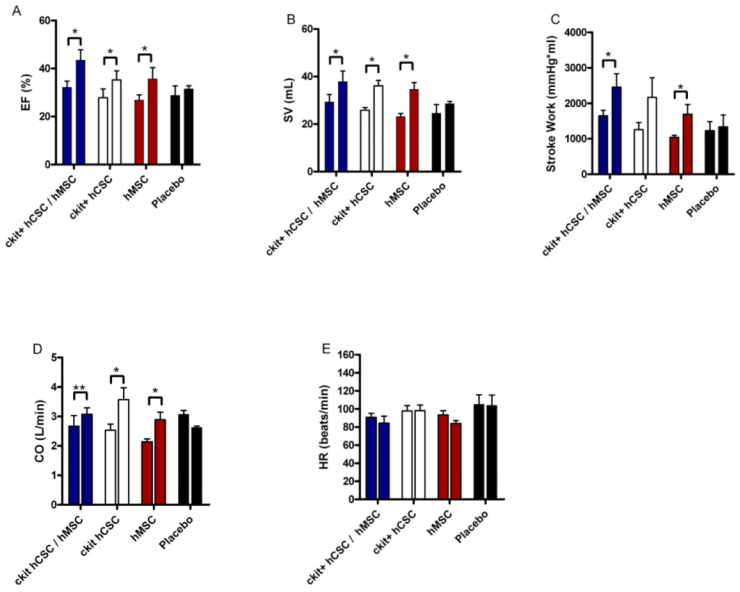

Figure 4.

Preload, afterload and contractility changes following hCSC and hMSC therapy. (A) Left ventricle end-diastolic pressure (LVEDP) and (B) end-diastolic volume (EDV) as well as afterload measured by (C) arterial elastance (Ea). Combination hCSC / hMSC therapy (n=5) improved contractility as measured by the (D) maximal rate of pressure change during systole (dP/dtmax) as well as (E) preload recruitable stroke work (PRSW), a preload independent measure of stroke work. There was no change in (F) systolic elastance (Ees), the slope of the end-systolic pressure volume relationship (ESPVR), in any of the groups. All graphs show pre-injection (2-weeks post-MI) vs. 4-weeks post-injection values. (*p<0.05 paired t-test; graphs represent mean±SEM)

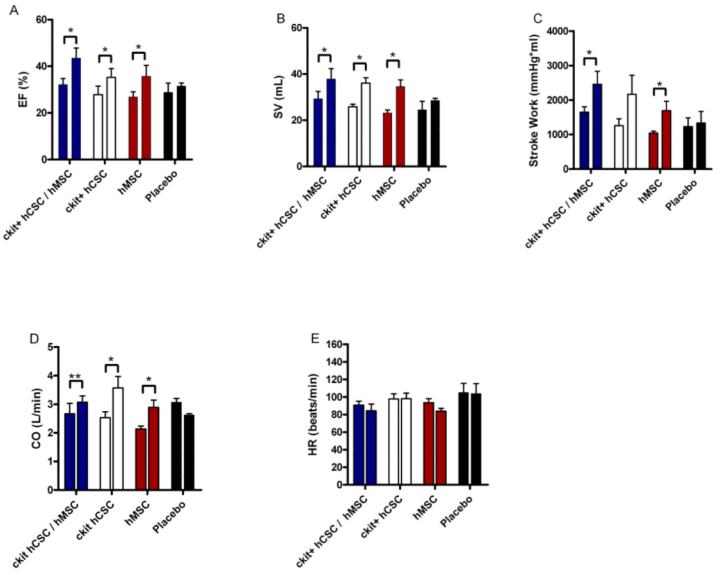

Figure 5.

Integrated measures of cardiac performance improve after hCSC and hMSC therapy. All stem cell treated groups demonstrated improved (A) ejection fraction (EF) and (B) stroke volume (SV), while the combination therapy (n=5) and hMSC alone therapy (n=5) improved (C) stroke work (SW), the area within the PV loop curve. The hMSC alone (n=5) and hCSC alone group (n=5) had improved (D) cardiac output (CO), while there was a trend towards improved CO in the combination therapy group (n=5; p=0.06). The placebo treated group (n=5) showed no change in any of the measures of integrated cardiac performance during follow-up, and all groups had unchanged (E) heart rate. All graphs show pre-injection (2-weeks post-MI) vs. 4-weeks post-injection values. (*p<0.05 and **p=0.06 paired t-test; graphs represent mean±SEM)

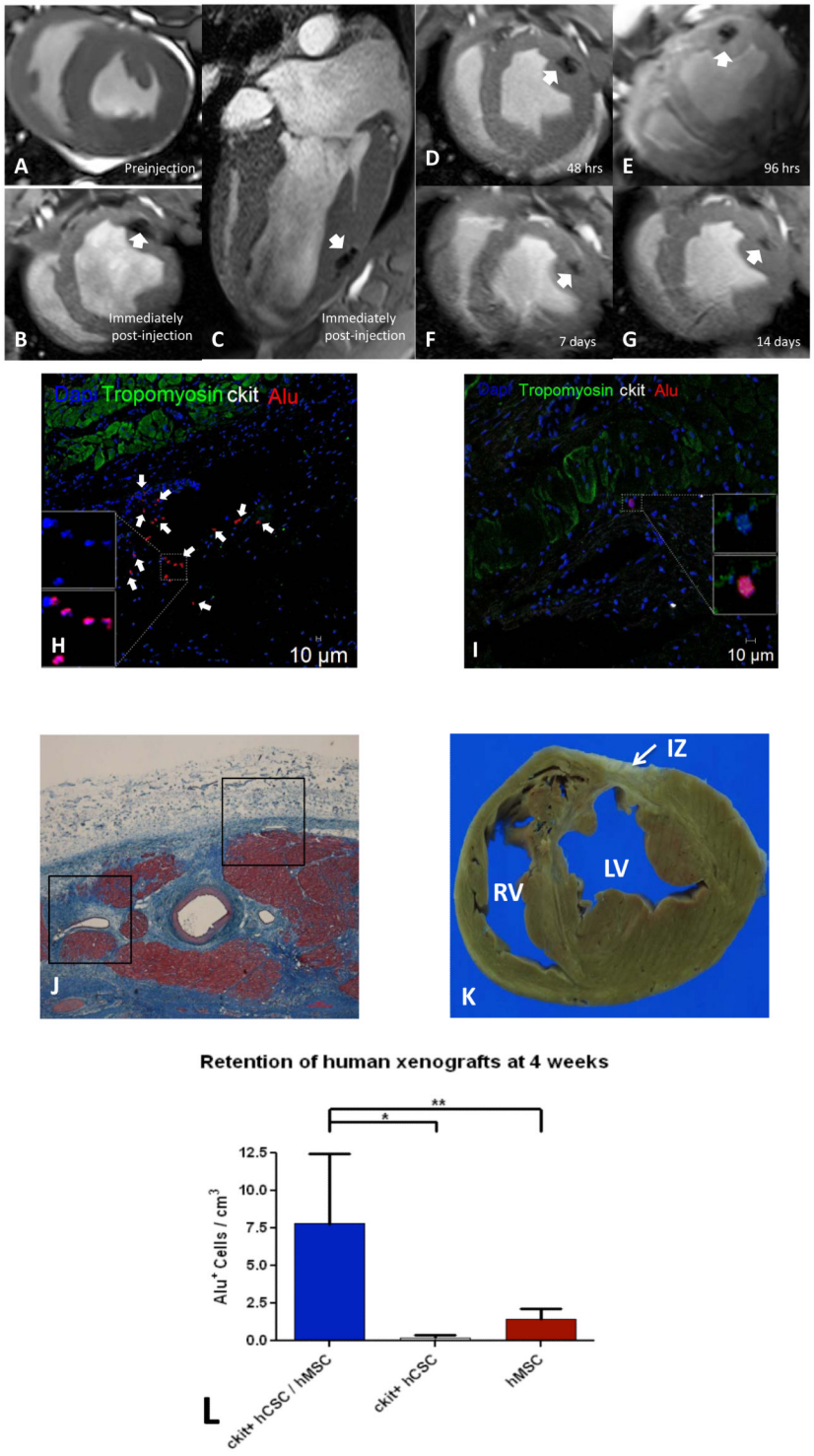

Figure 6.

Retention and engraftment and retention of human hCSCs and hMSCs in post-MI swine. (A-G) Cardiac MRI images showing retention of iron oxide labeled human stem cells by increased signal intensity (white arrow) in post-MI swine heart (representative of n=2). Immunohistochemical stained images showing clusters of Alu positive human stem cells

(white arrows) engrafted in the (H) infarct territory and (I) vasculature at 4-weeks post-transplantation. Engrafted human stem cells did not co-stain for c-kit. (J) Masson's trichome stained image depicting scar (blue) and islands of cardiomyocytes (red) with corresponding area of engraftment (black boxes) showing no cellular inflammation, which is also demonstrated in (K) gross section of heart (representative of n=5). (L) Retention of alu+ human stem cells was 7-fold higher when hCSCs and hMSCs were injected together compared to either cell type administered alone (n=3 analyzed per treatment group). (IZ =infarct zone, LV=left ventricle, RV=right ventricle;*$p<0.001$ and **$p<0.05$ between group one way ANOVA; graphs represent mean±SEM)

Table 1

Cardiac MRI Global Function and Scar Size

Parameter	Group	Baseline	2 weeks (pre-injection)	4 weeks	6 weeks	Overall within group p value
LV mass (g)	ckit+ hCSC / hMSC	67.4±10.50	77.9±9.51	93.5±16.41	98.6±18.89	0.001
	ckit+ hCSC alone	64.7±8.26	82.9±8.96	92.2±11.93	100.4±18.96	0.011
	hMSC alone	68.8±8.76	80.4±7.12	91.1±7.85	103.6±5.35	0.002
	Placebo	64.5±12.14	75.9±10.72	85.0±11.13	93.8±5.44	0.019
EDV (ml)	ckit+ hCSC / hMSC	66.5±8.49	93.1±11.99	97.7±12.23	95.0±14.90	0.481
	ckit+ hCSC alone	72.9±11.88	102±18.69	101.9±18.33	109.2±21.96	0.463
	hMSC alone	78.9±10.35	93.2±15.47	94.3±17.69	105.1±23.99	0.163
	Placebo	75.4±7.81	87.8±15.55	90.1±18.54	106.1±21.17 *	0.059
ESV (ml)	ckit+ hCSC / hMSC	38.7±7.35	61.2±7.98	56.8±11.95	53.0±7.91	0.141
	ckit+ hCSC alone	45.6±7/93	71.8±19.94	62.0±19.52	67.2±19.19	0.095
	hMSC alone	49.6±8.74	67.5±13.3	59.2±17.01	67.4±22.46	0.309
	Placebo	43.2±3.91	58.8±12.8	59.1±21.17	74.38±20.52 *	0.102
SV (ml)	ckit+ hCSC / hMSC	27.7±3.84	31.9±7.44	40.9±6.31	42.0±9.60	<0.001
	ckit+ hCSC alone	27.3±5.72	30.3±2.54	39.8±3.22	41.9±6.84	<0.001
	hMSC alone	29.3±4.51	25.6±2.76	35.0±5.84	37.9±6.20	<0.001
	Placebo	31.6±7.93	28.18±7.34	31.0±8.59	31.7±0.72	0.369
EF (%)	ckit+ hCSC / hMSC	41.9±5.48	34.1±5.69	42.2±7.02	43.8±5.4	<0.001
	ckit+ hCSC alone	37.4±4.82	30.8±7.74	40.3±9.01	39.3±8.36	<0.001
	hMSC alone	37.5±4.81	27.8±2.76	38.0±7.86	37.1±8.32	<0.001
	Placebo	41.5±6.86	32.38±7.02	35.4±12.17	30.0±4.61	0.945
Scar mass (g)	ckit+ hCSC / hMSC	0	14.1±2.40	12.3±2.66	11.2±2.58 †	<0.001
	ckit+ hCSC alone	0	14.1±3.57	13.2±2.96	12.5±2.85	0.006
	hMSC alone	0	13.8±2.74	12.0±1.77	12.4±2.51	0.015
	Placebo	0	15.1±6.95	16.1±8.02	17.2±6.83	0.430
Scar size (% LV mass)	ckit+ hCSC / hMSC	0	19.1±1.58	15.0±2.00	12.1±2.12 †	<0.001
	ckit+ hCSC alone	0	17.5±3.11	14.5±2.07	13.0±1.92	<0.001
	hMSC alone	0	17.8±3.11	14.3±1.55	13.5±2.61	<0.001
	Placebo	0	19.6±7.09	18.9±6.90	18.9±6.97	0.043

Values are mean±SD. Within and between groups repeated measures ANOVA compares pre-injection (2 weeks post-MI) vs. post-injection timepoints.

* p<0.05 within group repeated measures ANOVA at 6 weeks;

† p<0.05 combination hCSC/hMSC vs hMSC alone and hCSC alone between group repeated measures ANOVA at 6 weeks.